Response to reviewer Christian Borger:

We thank Christian Borger for his valuable review and the positive feedback of the manuscript. Below, we provide a point-to-point response to the comments and list the related changes made to the manuscript. The original review comments are shown in italic blue font, our responses are in regular black font, and new text added to the revised paper is indicated in red.

Major concerns from reviewer Christian Borger:

In recent years, important methodological improvements to flux-divergence-type emission estimates have been developed, but they are not reflected in the current manuscript. In particular, the following aspects should be considered and incorporated:

1. *Advection rather than divergence in the formulation (Beirle et al., 2023).*
2. *Topography-related corrections, which can be important in complex terrain (Sun, 2022).*

Beirle et al. (2023) neglect the wind divergence term and instead apply a topography correction separately to compensate the effects of the wind divergence due to orography. In contrast, our approach calculates the total flux divergence, which includes both the advection term and the wind divergence term. We calculate an effective wind field that compensates for the wind divergence. Wind divergence is mainly caused by vertical wind as a result of topography or land-sea crossing. By using the wind field corrected for wind divergence we indirectly compensate both for the wind divergence (which becomes negligble) and the topography related issue described by Sun (2022). Our approach is also detailed described and discussed in the study of Cifuentes Castaño et al. (2025). They have done the comparison by using the method from Beirle et al. (2023) and also the approach we used in our study and showed that the impact of topography is clearly reduced, especially along coastal regions by using our approach. Following the reviewer's suggestion, we have added more discussion on the divergence calculaton in Introduction.

In the manuscript, we add the following paragraph in the Introduction:

Recently, the flux-divergence method for emission estimation has been further refined. It is based on the steady-state continuity equation and estimated emissions are the sum of advection and chemical sink terms (Beirle et al., 2019). A topography correction was later introduced to compensate for terrain-

related biases in vertical column densities (VCDs) due to the vertical wind field (Sun, 2022), and has been applied to NO_x and CO emission estimation (Beirle et al., 2019; Sun, 2022). The topographic effects can also be accounted for by using total column densities (TVCDs) together with profile-weighted mean wind field for advection calculation (Koene et al., 2024). In addition, the previous studies also consider the full divergence (including both advection and wind divergence scaled by VCDs) for emission calculation. Sun (2022) demonstrates that the wind divergence term can be comparable in magnitude to a moderate emission signal. In this study, a corrected effective wind field is applied to reduce topographic influences and derive the NO_x and SO_2 emissions. (Chen et al., 2025; Cifuentes Castaño et al., 2025).

Except for the text added in "Introduction", we also add a sentence between line 115 and 116:

To reduce the artifacts from the simplified 2D wind field, especially occurring over complex terrain, we use the divergence-reduced wind field for the divergence calculation (Bryan, 2022)

3. *AMF-related consistency: it is currently unclear whether and how an AMF correction is applied. This matters especially because winds are referenced to a specific vertical level (e.g., PBL midpoint), and because plume height and vertical sensitivity can affect the effective column-to-mass conversion. The manuscript should clearly state the chosen approach (e.g., total column AMF or AMF at PBL midpoint).*

According to the COBRA SO_2 README file (https://data-portal.s5p-pal.com/product-docs/SO2cbr/S5P-BIRA-PRF-SO2CBR_1.0.pdf, last access: 19 Jan, 2026), the retrieved total column SO_2 VCDs used for the divergence calculation represent SO_2 pollution scenarios within the boundary layer. An air mass factor (AMF) appropriate for the boundary layer conditions has already been applied in the retrieval. However, there is still potential for further AMF improvement. The current surface albedo climatology used in the retrieval has a relatively coarse spatial resolution of 0.5° × 0.5° and a temporal resolution of one month. A refined AMF treatment could therefore improve the retrieval. We consider this an important direction for future work, but it is beyond the scope of this study.
Regarding the wind field, we use the wind speed at half of the planetary boundary layer height (PBL). This choice is based on the assumption that SO_2 is vertically well mixed within the PBL for the conditions relevant to our divergence analysis. Under this assumption, the wind at half of PBL provides a representative estimate of the mean transport conditions within the boundary layer.

We added a sentence in Section 2.1 in line 105:

The COBRA SO_2 VCDs represent SO_2 within Planetary Boundary Layer (PBL), mainly associated with anthropogenic emissions.

We added another sentence between line 113 and 116:

Assuming SO_2 is vertically well mixed within the PBL, we use horizontal wind fields at half of the PBL height to represent PBL wind conditions. To reduce the artifacts from the simplified 2D wind field, especially over complex terrain, we correct the 2D wind fields for the wind divergence following the method of Bryan (2022).

Swath-dependent pixel size and wind rotation, which can bias the derivative-based quantities and source shapes if ignored (Beirle et al., 2023).

We actually use the same wind-rotation method for the divergence calculation at the TROPOMI pixel level as described in Beirle et al. (2023) .

This has now been noted in Section 3.1 line 145:

We calculate the divergence on the TROPOMI pixels using the rotated wind field following the method of Beirle et al. (2023) and then interpolate the results on the regular grid cells of 0.025° × 0.025° for the final emission estimates for the best results.

Minor issues:

a. *Title: "High-resolution quantification" is potentially misleading. The conclusions correctly note that robust emission estimates require integration over a small area. A phrasing such as "super-resolution localization" would better reflect the main contribution.*

We thank the reviewer for this thoughtful observation. We agree that the phrase "high-resolution quantification" could be interpreted as emphasis on the calculation of Indian emissions rather than on the methodological improvement of pinpointing the emissions. To better reflect the content of our paper, we change the title to "*Super-resolution localization and quantification of SO_2 emissions over India using TROPOMI observations*"

b. *Section 2.1: Please clarify what is meant by the "midpoint of the PBL" and describe how the AMF is adjusted accordingly (or why no correction is needed).*

"Midpoint of the PBL" refers to the half of the PBL height. To avoid confusion, we have removed this term from the main text. According to the COBRA SO_2 README file (https://data-portal.s5p-

pal.com/product-docs/SO2cbr/S5P-BIRA-PRF-SO2CBR_1.0.pdf, last access: 19 Jan, 2026), the retrieved total column SO_2 VCDs used for the divergence calculation represent SO_2 pollution scenarios within the boundary layer. An air mass factor (AMF) appropriate for the boundary layer conditions has already been applied in the retrieval. However, there is still potential for further AMF improvement. The current surface albedo climatology used in the retrieval has a spatial resolution of 0.5° × 0.5° and a temporal resolution of one month, which is relatively coarse compared to the much finer resolution of individual S5P TROPOMI pixels. A refined AMF treatment could therefore improve the retrieval. We consider this an important direction for future work, but it is beyond the scope of this study.

Regarding the wind field, we use wind speed at half of the planetary boundary layer height (mid-PBL). This choice is based on the assumption that SO_2 is vertically well mixed within the PBL for the conditions relevant to our divergence analysis. Under this assumption, the wind at half of PBL provides a representative estimate of the mean transport conditions within the boundary layer.

c. *Section 3.1: The conclusion that derivatives should be computed on the native TROPOMI grid is well established (see de Foy and Schauer, 2022). Since the main value here is likely illustrative rather than novel, I suggest moving most of Section 3.1 to the appendix or supplement. In the main text, it may be more useful to expand the description of the divergence or advection computation, including practical details and assumptions.*

We move all the Section 3.1 with the basic descriptions to the supplementary file and we add more specific details on our method to this section.

In first paragraph of Section 3.1 in the manuscript, we added:

This full divergence calculation follows the method in Chen et al. (2025). Specifically, we use Eq. (S1) together with a corrected wind field to calculate SO_2 divergence. The wind is corrected using an iterative wind-divergence correction algorithm by Bryan (2022). As described in detail in Cifuentes Castaño et al. (2025) the impact of topography is clearly reduced, especially along coastal regions. We will calculate the emissions at various grid resolutions to test the effect of our sharpening: 0.1° × 0.1°, 0.05° × 0.05°, 0.025° × 0.025°, and 0.01° × 0.01°. We calculate the divergence on the TROPOMI pixels with rotated wind field following the method of Beirle et al. (2023) and then interpolate the results on the regular grid cells of 0.025° × 0.025° for the final emission estimates for the best results. See section S1 for more details.

d. Section 3.2: Please explain how B is constructed before presenting results in Figs. 2 and 3. When reading, the definition currently comes too late. Also specify the dimension of B (e.g., 5x5, 7x7). A figure showing the original kernel and the inverted kernel would help. Please also report the estimated noise level used for filtering.

We change the structure of the paper based on these comments. Now the spreading kernel information (Section 3.2) comes earlier than the sharpening algorithm description (Section 3.3). We also added the spreading kernel size (9×9) in Section 3.2. Instead of only using the five-year averaged emissions to derive the spreading kernel, we also use the individual annual emissions. We add the spreading kernel and the sharpening kernel in the supplementary file in Section S2.

Between line 154 to 167 in the manuscript, we added:

Kernel ***B*** can be derived from the derived emission distribution in the grid cells adjacent to the source location. Figure 1 shows the normalize derived SO_2 emissions as function of the distance from the point source location. To obtain a spreading kernel which represents the overall spreading pattern of point source emissions, we fit the emission variation around the large and isolated point sources in India using a Gaussian-shaped function. Figure 1a shows the SO_2 emissions and the corresponding Gaussian-shaped fitting functions as function of distance in kilometers. From Fig. 1a and Fig. S1, we see that the emission resolution improves with finer grid cells, but gains become marginal once the grid is finer than the TROPOMI pixel size. Figure 1b shows the SO_2 emission as function of distance from the point source location, but with distance expressed in grid cells. Since we decide to derive the SO_2 emissions based on TROPOMI pixels and regrid to 0.025° afterwards, we derive the spreading pattern from the corresponded Gaussian-shaped function (red dots in Fig. 1b) over the grid cells. The SO_2 emissions of point sources approaches zero at approximately 4 grid cells (around 11.25 km) away from the point sources. Therefore, we define the spreading region (also the size of the spreading kernel) for each point source as a 9 × 9 grid cells (around 22.5 km × 22.5 km) centered on the source location. The spreading kernel ***B*** follows a Gaussian-shaped function derived from the annual emissions with a sigma of 2.21 grid cells, and derived from five-year averaged emissions with the sigma of 1.83 grid cells. (See details in Section S2 in supplementary file).

e. Emission maps: Color bars should include negative values rather than stopping at 0. This can be diagnostically useful and may reveal, for example, topography-related artifacts.

We have added this figure in supplementary file.

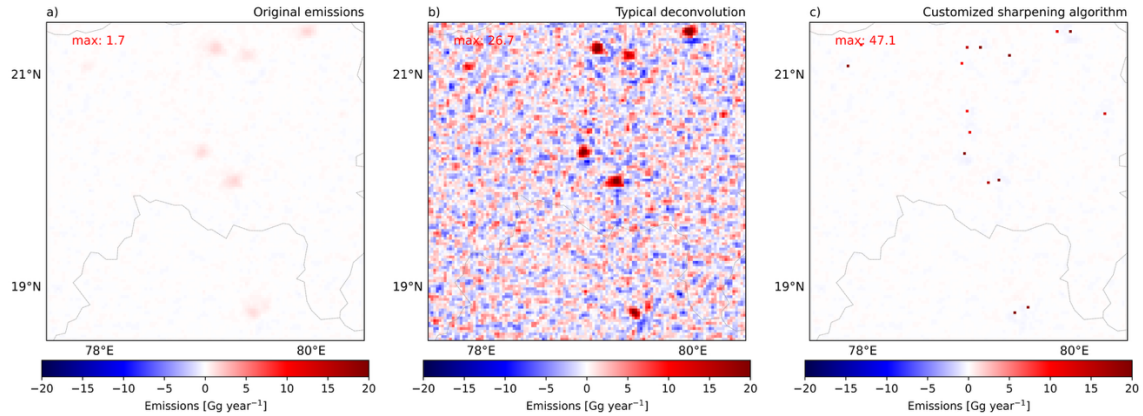

Figure S3. SO_2 emissions over a zoom-in region in India. a) Original SO_2 emissions. b) SO_2 emissions after the typical deconvolution. c) SO_2 emissions after customized sharpening algorithm (sharpening applied in descending order of emission).

Further questions

The analysis relies on multi-year mean SO_2 emission maps. How feasible would it be to apply the method to annual means? While the noise level would increase, this could enable analysis of temporal evolution such as commissioning of new facilities or shutdowns. Would monthly or quarterly averages be realistic, and what would the limiting factors be?

Following the comments, we update the analysis with both annual and five-year averaged results. Specifically, the Section 4.2 and 4.3 is based on annual results. And Section 4.4 and 4.5 are based on both annual and five-year averaged results. In addition, we also detect more point sources and added in Section 4.5.

As mentioned by the reviewer, short-term emission maps enable analysis of temporal changes, such as the commissioning of new facilities or shutdowns as mentioned by the reviewer. As long as the noise level is known, the emission signal can be clearly separated with the noise using our sharpening algorithm. We think the limiting factor is how accurate and representative the noise level is. We added the discussion related to this point mainly in Section 4.5.

In Section 4.5:

We find some new operating SO_2 point sources using both annual and five-year averaged SO_2 emission inventories. These emissions are absent in the Indian power plant database and are also not identified by the top-down SO_2 catalogue MSAQSO$_2$L4. These new point sources include not only coal-based power plants, but also cement factories, crude oil production facilities, a chemical fertilizer factory, and copper, steel, and aluminum industries. Table 2 provides the list and locations of these sources. Many newly detected sources are small and located close to known large point sources, but their weaker signals are distinguishable in our inventory. The annual emission inventory better distinguishes small point sources located near large ones, whereas the long-term averaged inventory provides more precise source locations. Most operating point sources show persistent SO_2 emission signal over five years. However, Rashtriya Chemicals Fertilizers (RCF) complex involving a sulphuric acid plant located in Trombay, Maharashtra is detected only for the year 2021. RCF reported that sulphur consumption in the financial year March 2021-March 2022 was 2.7 times higher than in 2020-2021 (https://www.rcfltd.com/public/storage/investers/1669721755.pdf, last access 20 Feb, 2026), indicating substantially higher potential SO_2 emissions in 2021.This indicates that applying the sharpening algorithm to short-term emission results enables the analysis of temporal variability, including emission changes and possible commissioning or shutdown events. In contrast, the Phil Coal Beneficiation and Sponge Iron Cluster is only detected in the five-year averaged inventory, but not in any individual annual result. This is because long-term averaging results reduces noises, allowing the sharpening algorithm to better detect small but stable emitters.

The conclusions mention transfer to NO_2. Would the authors suggest that this approach could also be applied to methane or are there any limiting factors (for example, lifetime, background variability, and retrieval characteristics)?

We tested the method using NO_x emissions, and the sharpening algorithm worked well for the point sources. We therefore expect it to also work for point-source emissions of other short-living species. For long-living species having a strong background concentration, like CH_4, we have not done any tests yet.

We mention this in Conclusion between line 354 and line 355:

Although this algorithm is developed for SO_2, it can also be applied to other short-lifetime pollutants emitted by point sources like NO_x. It helps sharpen emission signals on existing grid cells and is a useful step toward building accurate emission inventories. For long-living species having a strong background concentration, like CH_4, we have not done any tests yet.

Technical comments

The manuscript is difficult to read in places, particularly at the start of the introduction, and there are several sentence-level repetitions (for example in Section 3.2.2). A careful language edit would substantially improve clarity and flow. Given the list of experienced co-authors, this should be easily achievable.

Repetition in 3.2.2 is reduced and the text has been improved.

L14: second "instrument" at the end of the line is redundant.

Removed

L22: Does "6 km" refer to square kilometers? Please clarify.

On average 6 times 6 kilometers (Revised)

L53: Consider revising to "band of the electromagnetic spectrum."

Revised

L109: Please provide the DOI for the CAMS product.

Revised

L185: The symbol for epsilon differs from Eq. (6).

Revised

Figure 5: Please provide more details on the CAMS-GLOB-ANT-4.2 product.

Revised

Table 2: Are some of the listed sources still active?

Revised. And we also add more discussion about these sources

L481: Krol et al. is no longer a preprint. Please update the reference.

Revised

L531: "Steinfeld" should be "Seinfeld." ?

Revised.

References:

Beirle, S., Borger, C., Jost, A., and Wagner, T.: Catalog of NO_x point source emissions (version 2), World Data Center for Climate (WDCC) at DKRZ [dataset], 10.26050/WDCC/No_xPointEmissionsV2, 2023.

Beirle, S., Borger, C., Dörner, S., Li, A., Hu, Z., Liu, F., Wang, Y., and Wagner, T.: Pinpointing nitrogen oxide emissions from space, Sci. Adv., 5, eaax9800, doi:10.1126/sciadv.aax9800, 2019.

Bryan, L.: The Flux Divergence Method Applied to Nitrogen Emissions in The Netherlands, Master thesis, TU Delft Electrical Engineering, Mathematics and Computer Science, Delft University of Technology, 2022.

Chen, Y., van der A, R. J., Ding, J., Eskes, H., Williams, J. E., Theys, N., Tsikerdekis, A., and Levelt, P. F.: SO2 emissions derived from TROPOMI observations over India using a flux-divergence method with variable lifetimes, Atmos. Chem. Phys., 25, 1851-1868, 10.5194/acp-25-1851-2025, 2025.

Cifuentes Castaño, F., Eskes, H., Dammers, E., Bryan, C., and Boersma, K.: Accurate space-based NOx emission estimates with the flux divergence approach require fine-

scale model information on local oxidation chemistry and profile shapes, Geoscientific Model Development, 18, 621-649, 10.5194/gmd-18-621-2025, 2025.

Koene, E. F. M., Brunner, D., and Kuhlmann, G.: On the Theory of the Divergence Method for Quantifying Source Emissions From Satellite Observations, J. Geophys. Res. Atmos., 129, e2023JD039904, https://doi.org/10.1029/2023JD039904, 2024.

Sun, K.: Derivation of Emissions From Satellite-Observed Column Amounts and Its Application to TROPOMI NO2 and CO Observations, Geophys. Res. Lett., 49, e2022GL101102, https://doi.org/10.1029/2022GL101102, 2022.